Experimental Study of RC Frame Infilled with Opening Brick Wall

Shuenn-Yih Chang [1,*], Guo-Chen Hsu [1], and Chiu-Li Huang [2]

[1] National Taipei University of Technology, Taipei, Taiwan
[2] Fu Jen Catholic University, New Taipei City, Taiwan; Email: 003951@mail.fju.edu.tw (C.L.H.)
*Correspondence: changsy@ntut.edu.tw (S.Y.C.)

***Abstract*—A total of three reinforced concrete bare frames infilled with brick walls were cyclically tested in this study. Each frame was infilled with a different shape of brick wall. A cyclically loading test was conducted for each specimen so that the hysteretic behaviors as well as the evolution of the failure mode of each specimen can be revealed, especially for the different shape of the infilled brick wall. In fact, the hysteretic behaviors of each specimen can be disclosed by examining the variations of the hysteretic loops of lateral forces-lateral displacement relationships while the evolution of the failure mode of each specimen can be manifested from the test procedure. There was no short column failure of the side column for each specimen although it was constrained by the infilled brick wall. It is affirmed that the stair-step crack pattern is generally consistent with the diagonal force transfer mechanism of brick walls.**

***Keywords*—reinforced concrete frame, opening brick wall, infilled brick wall, diagonal force transfer mechanism, cyclic loading test**

I. Introduction

Three shapes of brick walls are very often experienced in reinforced concrete frames infilled with brick walls in Taiwan [1–5]. One is a reinforced concrete frame infilled with a full brick wall, where each side of the brick wall is constrained and the other is a reinforced concrete frame infilled with an opening brick wall, where a door is next to the column. Clearly, only three sides of the brick wall are constrained. A reinforced concrete frame infilled with a top opening brick wall is the third shape and it is a very common design for a rest room in Taiwan area since it can give natural lighting and ventilation the movement of fresh air. Notice that some other shapes of infilled brick walls can still be found in the existing reinforced concrete structures. Some reinforced concrete frames infilled with specific shapes of brick walls, such as a top opening brick wall and a full brick wall have been cyclically loading tested [2, 4]. However, these tests are very rare. Besides, there exist no related papers or reports in the literature for other shapes of infilled brick walls for reference purpose. Hence, it becomes a difficult job for practical engineers to conduct a pushover analysis for the seismic evaluation of existing structures with these shapes of infilled brick walls. Therefore, it is useful to conduct cyclically loading tests of reinforced concrete frames infilled with some specific shapes of brick walls [6].

Three identical reinforced concrete frames infilled with three different shapes of brick walls were fabricated and then a series of cyclically loading tests were performed in this experimental study. It is important to look into the evolution of the failure mode of each specimen during the test. Besides, the hysteretic behaviors of each specimen can be revealed by examining its hysteretic loops. Finally, it is important to identify the mechanism of the diagonal force transfer so that a properly compressive bracing can be applied to mimic each brick wall and then a pushover analysis of reinforced concrete frame with these shapes of brick walls can be reliably conducted [7–12].

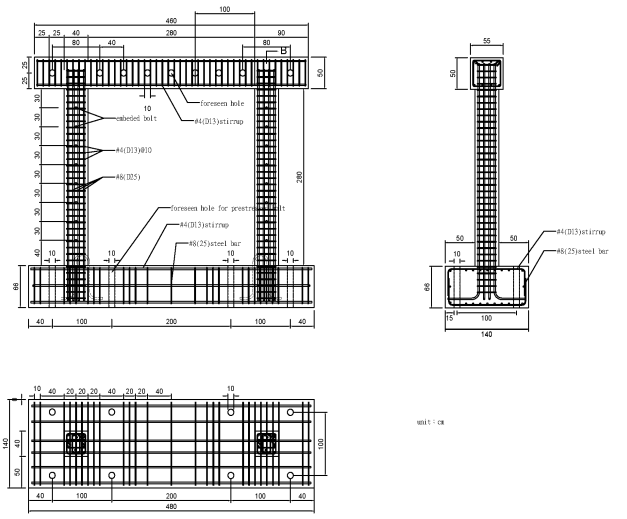

Figure 1. Design details for RC frames.

II. Fabrication of Specimens

Three reinforced concrete frames with three different shapes of brick walls were fabricated for the cyclically loading tests. Fig. 1 shows the design details of the three identical reinforced concrete bare frames. The total height of the frame is 396cm and net height of the columns is 280cm. The cross section of the column is 40×40cm and that for the beam is 50×55cm. Notice that the adoption

Manuscript received February 8, 2023; revised March 22, 2023; accepted May 29, 2023.

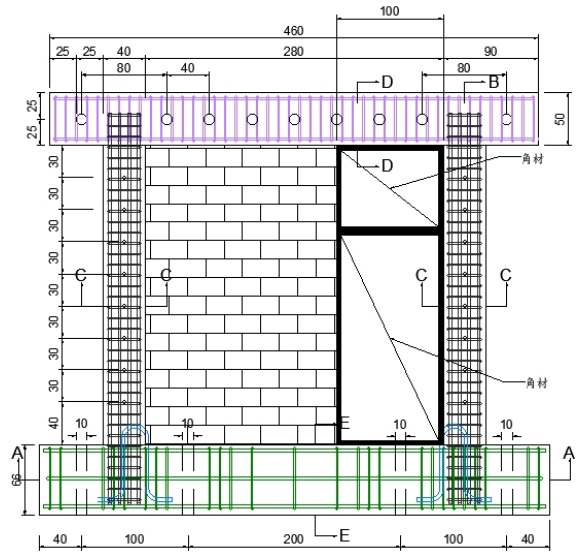

(a) Specimen S1

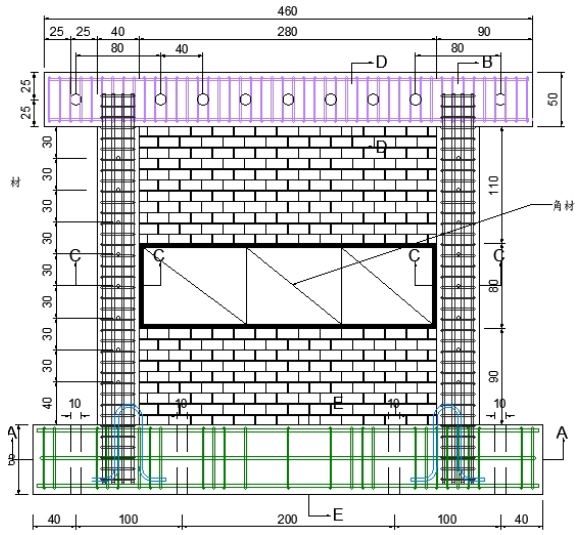

(b) Specimen S2

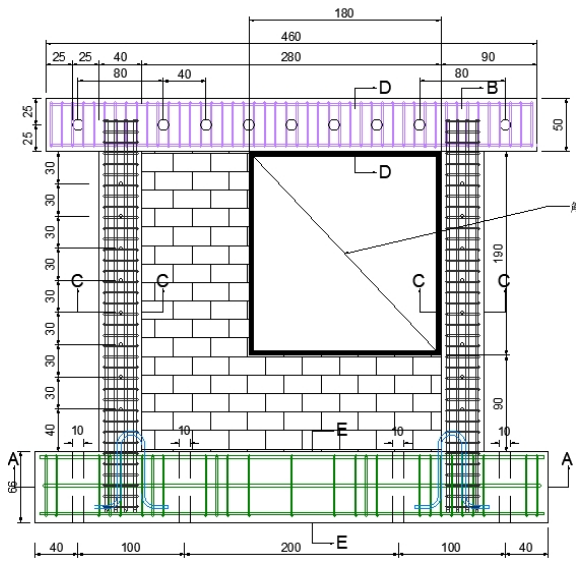

(c) Specimen S3

Figure 2. Three RC frames infilled with different types of brick walls for S1, S2 and S3.

of a large cross section of the beam is intended to mimic a rigid beam so that each side column can have a double curvature bending. The three different shapes of infilled brick walls can be manifested from Fig. 2, where S1, S2 and S3 are introduced to represent the three specimens of reinforced concrete frames infilled with shape 1, shape 2 and shape 3 brick wall, respectively. The brick bonding pattern of the Flemish bond was adopted for each infilled brick wall. It should be mentioned that the bricklaying method as shown in each plot of Fig. 2 does not denote the realistic brick bonding pattern of each specimen and it is just used to simply illustrate the shape of the opening of each brick wall.

The material property of reinforcing bars for #4 steel rebar is 2800kgf/cm^2 kgf / cm^2 while for #8 steel rebar is 4200 kgf / cm^2 for the yielding design strength. Besides, the compressive design strength of the concrete is chosen as 280 kgf / cm^2 . On the other hand, it was experimental obtained that the yielding strength for #4 steel rebar is 3310 kgf / cm^2 while for #8 steel rebar is 4950 kgf / cm^2 . In addition, the compressive test strength of the concrete is found to be 326 kgf / cm^2 .

Figure 3. Test setup.

III. Test Setup

As is shown in Fig. 3, a fabricated reinforced concrete frame infilled with brick walls was fixed into a strong steel frame by connecting its foundation to a strong floor. Two hydraulic actuators were installed at the both sides of the frame for lateral loading of the frame at the beam's mid-height. Besides, two load cells were used to measure the applied lateral loads to the steel frames and the lateral displacement of the steel frame was measured by a Linear Variable Differential Transformer (LVDT) at the mid-height of the top beam of the steel frame [13, 14]. Each specimen was subjected to a quasi-static cyclically loading that was recommended by FEMA 461 [15]. The loading sequence as shown in Fig. 4 is composed of a

series of repeated cycles that have the characteristic of step-wise increasing deformation amplitudes. According to FEMA 46, the number of steps for cyclic loading tests in the loading sequences should be ten or more, and two cycles must be conducted at each step.

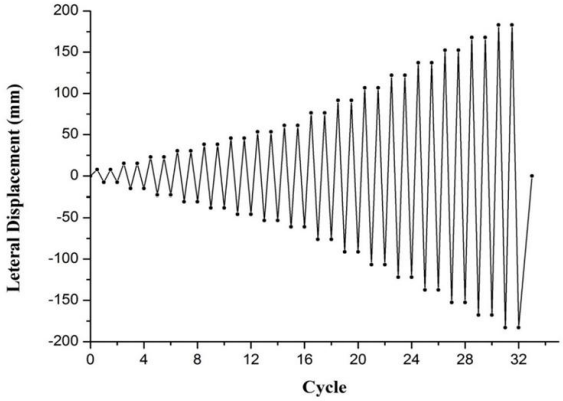

Figure 4. Applied loading sequences.

IV. Cyclic Loading Test

A series of cyclic loading tests were performed for S1, S2 and S3. In addition to obtaining the hysteretic loop for each specimen, the evolution of the different failure mode of each shape of infilled brick wall will be also addressed.

A. S1 Specimen

The development of crack pattern of S1 is shown in Fig. 5. Only very small horizontal flexural tensile cracks appeared at the top of columns at the inter-story drift ratio of 0.25%. Notice that there was no crack in the brick wall at this inter-story drift ratio. As the inter-story drift ratio reached 0.50%, an inclined crack was initated at the left-bottom corner of the brick wall and it propagated upward and rightward gradually to about half-width of the brick wall. Subsequently, this crack became a bed-joint sliding opening when it propagated to the right brick wall. At the inter-story drift ratio of 1.00%, the width of the first crack increased significantly. Besides, a new inclined crack was found right above the first crack. Evidently, two diagonal cracks of the brick wall were formated and intersected at the center of the brick wall as the inter-story drift ratio of 1.50% was reached. Therefore, the diagonal force transfer mechanism was clearly established. Some splitting cracks and crushed bricks were found around the four corners of the brick wall.

As the lateral displacement increased, multiple inclined diagonal cracks of the brick wall were found. In addition, more splitting cracks and crushed bricks were visible near the four corners of the brick wall, as the inter-story drift ratio of 2.50% was imposed. In this drift ratio, the infilled brick wall reached its maximum lateral strength. After the maximum lateral strength was achieved, cracks continued to grow and expand along the main path of the stair-step cracking, and new cracks were also developed in intact sections of the brick wall until a large quantity of bricks were crushed and disintegrated as the inter-story drift ratio of 3.00% was reached. As a result, the brick wall was collapsed as shown in Fig. 5(e).

It is manifested from Fig. 5(c) that the mechanism of diagonal force transfer was clearly formatted in the brick wall. Hence, it seems appropriate to adopt a compressive bracing to mimic an infilled brick wall under compressive loading as indicated in Fig. 5(c).

(a) Inter-story drift ratio of 0.50%

(b) Inter-story drift ratio of 1.00%

(c) Inter-story drift ratio of 1.50%

(d) Inter-story drift ratio of 2.50%

(e) Inter-story drift ratio of 3.00%

Figure 5. Development of crack pattern of S1.

B. S2 Specimen

Fig. 6. shows the development of crack pattern of S2. It is seen that there was almost no crack in the brick wall before the inter-story drift ratio of 0.50%. An inclined stair-step crack was initated from the left-bottom corner of the top brick wall and then it propagated upward and rightward to the bottom of the beam as the inter-story drift ratio was 0.50%. A new inclined stair-step crack was found and almost parallel to the first inclined stair-step crack at the inter-story drift ratio of 0.75%. Both inclined stair-step cracks continued to growth and more splitting cracks occurred in the central area of the top brick wall as inter-story drift ratio reached 1.00% as shown in Fig. 5(b).

At the inter-story drift ratio of 2.00%, splitting cracks continued to grow in the top brick wall and an inclined stair-step crack was initiated from the left-bottom corner and it propagated rightward and upward gradually. It is seen in Fig. 5(d) for the inter-story drift ratio of 3.00%, the width of the two inclined stair-step crack increased and vertical cracks were also found in the right part of the top brick wall. A new inclined stair-step crack was found in the bottom brick wall. The maximum lateral strength of S2 was reached at this drift ratio. At the inter-story drift ratio of 5.00%, some bricks near to each side column for both top and bottom brick walls were crushed.

It is evident that the top brick wall experienced more severe damage in contrast to the bottom brick wall. It is also found that the crack pattern of the top brick wall is also different from that of the bottom brick wall. It seems that either top or bottom brick wall can be simulated by two diagonal bracings as shown in Fig. 5(c).

(a) Inter-story drift ratio of 0.50%

(b) Inter-story drift ratio of 1.00%

(c) Inter-story drift ratio of 2.00%

(d) Inter-story drift ratio of 3.00%

(e) Inter-story drift ratio of 5.00%

Figure 6. Development of crack pattern of S2.

C. S3 Specimen

Both the development of crack pattern and evolution of failure of S3 are plotted in Fig. 7. For the convenience of the subsequent discussions of S3, the L-shape brick wall is divided into a top brick wall and a bottom brick wall by a red line as shown in Fig. 7(a). At the inter-story drift ratio of 0.50%, there was an inclined stair-step crack from the left-bottom to right-top of the top brick wall. Besides, a horizontal crack was discovered in the mid-height of the bottom brick wall and it propagated to the right-bottom of the brick wall as shown in Fig. 7(a). At the inter-story drift ratio of 1.00%, the inclined stair-step crack grew and expanded. Some splitting cracks were found in the left-bottom of the top brick wall in addition to some crushed bricks. It is evident that the mechanism of the diagonal force transfer was formatted for the top brick wall. The stair-step cracking in the bottom brick wall also became more significant.

In Fig. 7(c), the cracking pattern implies that it seems more appropriate to divide the L-shape brick wall into two small brick walls by a vertical red line as shown in this plot. Hence, one can find that a new inclined stair-step crack started to gradually propagate from the left-top to the right-bottom of the top brick wall at the inter-story drift ratio of 1.50%. More splitting cracks and crushed bricks was also found around the central area of the right brick wall. In Fig. 7(e), at the inter-story drift ratio of 2.50%, an inclined stair-step crack was clearly formatted from the left-top to right-bottom of the right brick wall while another inclined stair-step crack was formatted in the middle part of the right brick wall and started form its left-bottom to right-top. Thus, it seems that the diagonal force transfer mechanism can be used to model both stair-step cracking curves. In fact, a compressive bracing of AB can be used to represent the diagonal force transfer mechanism as a lateral force is loaded in a direction from left to right while a compressive bracing of CD can be used to denote the diagonal force transfer mechanism as a lateral force is imposed upon S3 in a direction from right to left.

(a) Inter-story drift ratio of 0.50%

(b) Inter-story drift ratio of 1.00%

(c) Inter-story drift ratio of 1.50%

(d) Inter-story drift ratio of 2.00%

(e) Inter-story drift ratio of 2.50%

Figure 7. Development of crack pattern of S3.

V. Hysteresis Loops of Load–displacement Relationship

After conducting the cyclically loading testing of S1, S2 and S3, the hysteretic loops of the force-displacement relation for each specimen are plotted in Figs. 8–10 for S1, S2 and S3, respectively. In this work, the lateral force is the total force applied by the two actuators and the lateral displacement the specimen is an average value of the values measured from the two LVDTs. Besides, in each figure, the yielding point, maximum lateral force point and ultimate lateral force point were marked, where the ultimate lateral force was taken to be the 80% of the maximum lateral force [16–22]. In this study, an average value is generally calculated from the two values in the push and pull directions, such as $\delta_y = (\delta_y^+ + \delta_y^-)/2$. In addition, as can be seen in Figs. 8 to 10, the major resistant brick wall of each specimen was destroyed while the two side columns can still remain stable at the end of the test. It seems that the yielding point as shown in Figs. 8–10 for S1 to S3 generally occurred as the major resistant brick wall was severely destroyed for each specimen.

A. S1 Specimen

An average yielding displacement of $\delta_y = 26.97$ mm with an average lateral yielding strength of 465.94 kN can be found from Fig. 8. Besides, an average maximum lateral strength of 579.83 kN is also found. Meanwhile, an average ultimate lateral strength is 449.22 kN and its corresponding average ultimate displacement is found to be $\delta_u = 137.75$ mm. As a result, the ductility of S1 is of $\delta_u / \delta_y = 5.11$.

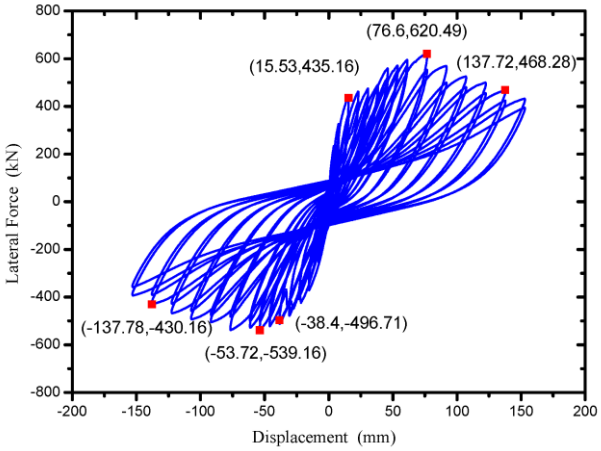

Figure 8. Force-displacement hysteretic loops for S1.

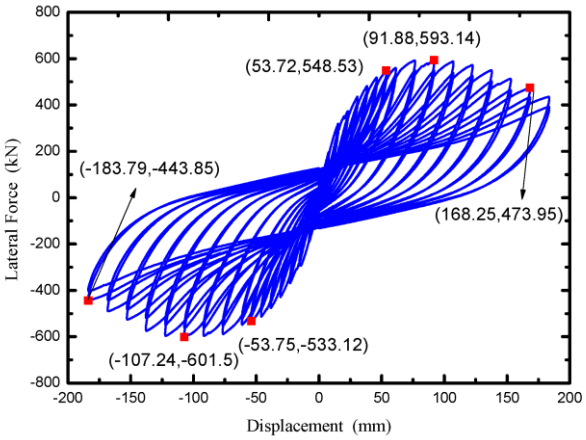

Figure 9. Force-displacement hysteretic loops for S2.

B. S2 Specimen

It is manifested from Fig. 9 that the average yielding displacement is $\delta_y = 53.74$ mm and the average lateral yielding force is 540.83 kN. An average maximum lateral force is found to be 597.32 kN and the average ultimate lateral force is 458.90 kN. Besides, the average ultimate displacement is found to be $\delta_u = 176.02$ mm. Hence, the ductility of S2 can be computed by δ_u / δ_y and is found to be 3.28.

C. S3 Specimen

An average yielding displacement of $\delta_y = 30.79$ mm is found for S3 in Fig. 10 and an average corresponding lateral yielding force is 460.70 kN. It is also revealed by

this figure that the average maximum lateral force is 567.13 kN and an average ultimate lateral force of 430.61 kN is identified. Thus, an average corresponding ultimate displacement is found to be $\delta_u = 153.01$ mm. As a result, one can have the ductility of $\delta_u / \delta_y = 4.97$.

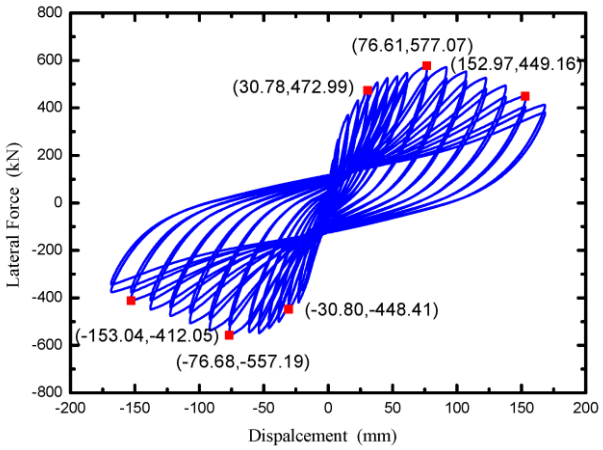

Figure 10. Force-displacement hysteretic loops for S3.

D. Comparison

It is of interest to compare the hysteretic behaviors of S1, S2 and S3. For this purpose, the important values of the test results of each specimen are abstracted and listed in Table I. Besides, the capacity curve of each specimen is summarized in Fig. 11 and the lateral stiffness of each hysteretic loop is also calculated and the variation of this calculated lateral stiffness with its corresponding lateral displacement is plotted in Fig. 12.

TABLE I. COMPARISON OF HYSTERETIC BEHAVIORS FOR S1, S2 AND S3

Specimen	Yielding displacement $\delta_y (mm)$	Yielding strength (kN)	Max lateral strength (kN)	Ult lateral displacement $\delta_u (mm)$	Ult lateral strength (kN)	$\mu = \delta_u / \delta_y$
S1	26.97	465.94	579.83	137.75	449.22	5.11
S2	53.74	540.83	597.32	176.02	458.90	3.28
S3	30.79	460.70	567.13	153.01	430.61	4.97

It is evident that the applied lateral force was resisted by the two side columns and infilled brick walls. Since a relatively large cross section was designed for the two side columns, the infilled brick walls were failed before the two columns. As a consequence, the hysteretic loops look similar to each other as demonstrated in Figs. 8–10. However, differences are still found due to the infill of the different shapes of brick walls. Evidently, the shape of two horizontal brick walls of S2 can possess the largest capacity to resist the lateral force while the L-shape brick wall of S3 has the smallest capacity. This is manifested from Table I and Fig. 11. It is also disclosed by Fig. 11 that the shape of two horizontal brick walls for S2 also leads to a better performance under cyclic loading test in contrast to the other two specimens. On the other hand, it is disclosed by Fig. 12 that S1 can have the largest initial lateral stiffness while S2 has the smallest initial lateral stiffness. This might be because that both S1 and S3 were infilled with the brick wall that is from the bottom to top of the reinforced concrete frame although it is an opening brick wall. It is also found that all the specimens all result in almost the same lateral stiffness after the failure of the infilled brick walls. In fact, after the failure of the infilled brick walls, the lateral force is generally resisted by the bare frame for each specimen.

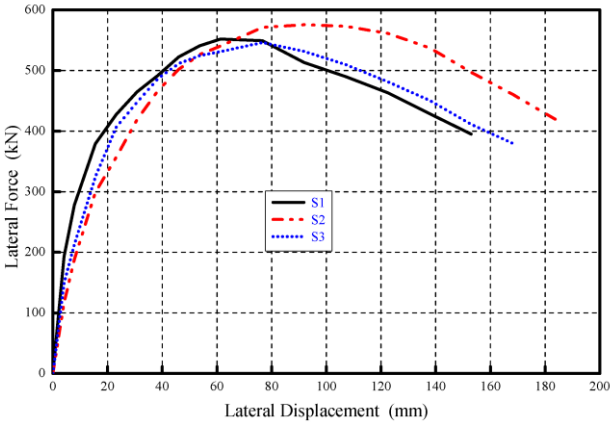

Figure 11. Capacity curves for S1, S2 and S3.

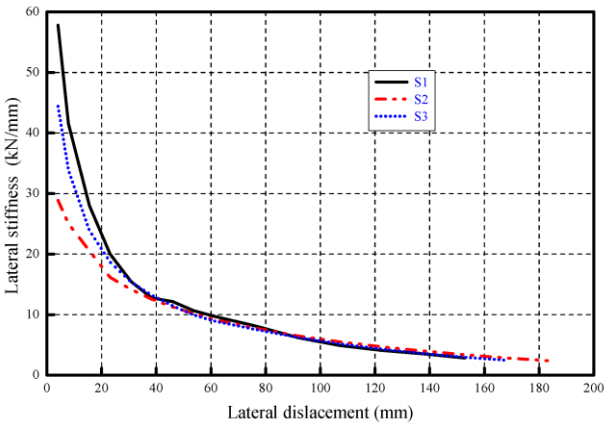

Figure 12. Variation of lateral stiffness with lateral displacement for S1, S2 and S3.

VI. CONCLUSIONS

In this experimental study, a total of three reinforced concrete bare frames infilled with three different shapes of brick walls were cyclically tested. The evolution of the failure mode of each specimen can be manifested from the cyclically loading test. In addition, the stair-step cracking of each brick wall can reveal the mechanism of diagonal force transfer and thus it can be appropriately simulated by a compressive bracing. It is evident that two diagonal force transfer mechanisms were formatted for S1 in the two diagonal directions of the infilled brick wall. Similar phenomena are also found for the top and bottom infilled brick walls of S2. Unlike the phenomena found for S1 and S2, although there were diagonal force transfer mechanisms for S3 in the two diagonal directions of the right infilled brick wall, one is from the left-top corner to the right-bottom corner in the right brick wall while the other is clearly formatted in the middle part of the right brick wall from the left-bottom corner to right-top corner.

To further substantiate that the use of a compressive bracing to simulate a diagonal force transfer mechanism for an infilled brick wall can lead to an accurate pushover analysis, a pushover analysis of each specimen is under investigation and the calculated capacity curve will be further compared to the cyclic loading test result so that the correctness of the analysis can be justified. All the analytical results of this study will be published later and somewhere.

CONFLICT OF INTEREST

The authors declare no conflict of interest.

AUTHOR CONTRIBUTIONS

S. Y. Chang conducted the research and wrote the paper; the experimental works were carried by G. C. Hsu and all the data of the paper were prepared by C. L. Huang. All authors had approved the final version.

FUNDING

This study was financially supported by the Grant No. MOST-110-2221-E-027-020 of the Ministry of Science and Technology, Taiwan.

REFERENCES

[1] C. P. Hsiao, H. H. Yeh, M. S. Sheu, K. C. Tsai, and Y. Q. Ding, *General Report on Damage in Chi-Chi Earthquake-damage Investigation for Building Structures*, Report No. NCREE-99-054, National Center for Research on Earthquake Engineering: Taipei, Taiwan, 1999. (In Chinese)

[2] Y. H. Chen. *Seismic Evaluation of RC Buildings Infilled with Brick Walls*, Doctoral dissertation, National Cheng Kung University: Tainan, Taiwan, 2003. (In Chinese)

[3] L. L. Chung, Y. K. Yeh, W. Y. Chien, F. P. Hsiao, W. C. Shen, T. C. Chiou, T. K. Chow, Y. F. Chao, Y. S. Yang, Y. S. Tu, J. F. Chai, S. J. Hwang, and C. H. Sun, *Technology Handbook for Seismic Evaluation and Retrofit of School Buildings* (Second Edition). Report No. NCREE-09-023, National Center for Research on Earthquake Engineering: Taipei, Taiwan, 2009. (In Chinese)

[4] M. S. Sheu, Y. H. Chen, and H. Y. Kuo, *Seismic Assessment of RC Street Buildings with Brick Walls*, First EQTAP Hazard Assessment and Structural Mitigation Workshop, Tokyo, Japan, 2003.

[5] M. S. Sheu, T. Kubo, and H. Y. Kuo, "Seismic Evaluation and Its Verification of Street Buildings in Taiwan," in *Proc. the 13th World Conference on Earthquake Engineering (13WCEE)*, Vancouver, B.C., Canada, 2004.

[6] Construction and Planning Agency of Taiwan. *Design and Construction Code for Masonry Buildings*, Ministry of the Interior: Taipei, Taiwan, 2008. (in Chinese)

[7] N. Hori, N. Inoue, D. Purushotam, T. Nishida, and J. Kobayashi. "Experimental and analytical studies on earthquake resisting behaviour of confined concrete block masonry structures," *Earthquake Engineering and Structural Dynamics*, vol. 35, no. 13, pp. 1699-1719, 2006.

[8] R. Meli, "Structural design of masonry buildings: The Mexican practice," *ACI Special Publication*, vol. 147, pp. 239-262, 1994.

[9] L. Garc á and L. Yam ń, "Review of masonry construction in Colombia," *ACI Special Publication*, vol. 147, pp. 283-305, 1994.

[10] R. Meli, S. Brzev, M. Astroza, T. Boen, F. Crisafulli, J. Dai, M. Farsi, T. Hart, A. Mebarki, A. S. Moghadam, D. Quiun, M. Tomazevic, and L. Yamin, *Seismic Design Guide for Low-rise Confined Masonry Buildings*, Earthquake Engineering Research Institute (EERI): Oakland, USA, pp. 1-90, 2011.

[11] A. Stavridis, I. Koutromanos, and P. B. Shing, "Shake-table tests of a three-story reinforced concrete frame with masonry infill walls," *Earthquake Engineering and Structural Dynamics*, vol. 41, no. 6, pp. 1089-1108, 2012.

[12] A. San Bartolome, J. Bernardo, and M. Pe ña, "The effect of column depth on seismic behavior of confined masonry walls," *Chilean Conference on Seismology and Earthquake Engineering*, Valdivia-Santiago, Chile, 2010.

[13] S. Y. Chang and S. A. Mahin, "Two new implicit algorithms of pseudodynamic test methods," *Journal of the Chinese Institute of Engineers*, vol. 16, no. 5, pp. 651-664, 1993.

[14] S. Y. Chang, "An explicit structure-dependent algorithm for pseudodynamic testing," *Engineering Structures*, vol. 46, pp. 511-525, 2013.

[15] ACI Committee 374.1-05. *Acceptance Criteria for Moment Frames Based on Structural Testing and Commentary*, Report Number 374.1-05, Ameriacn Concrete Institute: Farmington Hills, Michigan, pp. 1-9, 2005.

[16] T. Paulay and M. J. N. Priestley, *Seismic Design of Reinforced Concrete and Masonry Buildings*, Wiley: New York, pp. 584-594, 1992.

[17] ASCE/SEI-41. *Seismic Rehabilitation of Existing Buildings Supplement No. 1*, American Society of Civil Engineers: Reston, Virginia, pp. 145-225, 2007.

[18] S. Y. Chang, T. W. Chen, N. C. Tran, and W. I. Liao, "Seismic retrofitting of RC columns with RC jacketing and wing walls for using different structural details," *Earthquake Engineering and Engineering Vibrations*, vol. 13, no. 2, pp. 279-292, 2014.

[19] S. Y. Chang, "Bi-directional pseudodynamic testing," *Journal of Engineering Mechanics*, ASCE, vol. 135, no. 11, pp. 1227-1236, 2009.

[20] S. Y. Chang and I. C. Tsai, "Experimental study of as-built and composite materials retrofitted reinforced concrete columns," *Canadian Journal of Civil Engineering*, vol. 32, no. 2, pp. 454-460, 2005.

[21] S. Y. Chang, Y. F. Li, and C. H. Loh, "Experimental study of seismic behaviors of as-built and carbon fiber reinforced plastics repaired reinforced concrete bridge columns," *Journal of Bridge Engineering*, ASCE, vol. 9, no. 4, pp. 391-402, 2004.

[22] S. Y. Chang, T. W. Chen, and C. Y. Yang, "Pseudodynamic technique to obtain reliable shock response," *International Journal of Structural Stability and Dynamics*, vol. 14, no. 1, 1350050-1~27, 2014.